Proceedings of the

SYMPOSIUM ON RECENT ADVANCES IN GEOTECHNICAL CENTRIFUGE MODELING

A symposium on Recent Advances in Geotechnical Centrifuge Modeling was held on July 18-20, 1984 at the University of California at Davis. The symposium was sponsored by the National Science Foundation's Geotechnical Engineering Program and the Center for Geotechnical Modeling at the University of California at Davis.

The symposium offered an opportunity for a meeting of the International Committee on Centrifuges of the International Society for Soil Mechanics and Foundation Engineering. The U.S. participants also met to discuss the advancement of the centrifuge modeling technique in the U.S. A request is being transmitted to the American Society of Civil Engineers to establish a subcommittee on centrifuges within the Geotechnical Engineering Division.

An investigation of the Bearing Capacity of Footings under eccentric and inclined loading on Sand in a Geotechnical Centrifuge

by R. G. James* and H Tanaka†

* Assistant Director of Research, Cambridge University Engineering Dept.

† Senior Research Engineer, Port & Harbour Research Institute, Yokosuka, Japan

Abstract

The results of centrifuge model tests on the behaviour of flat and conical footings on dense sand are reported and compared with the standard bearing capacity formulae for veritcal, horizontal and eccentric loading.

Introduction

The work reported in the paper is part of an SERC research program conducted at the C.U.E.D. in relation to the behaviour of conical foundations (spuds) of Jack-up platforms. This program covers the behaviour of plane circular footings and conical footings on sand and on thin layers of sand overlying soft clay - however the results reported here will be mainly confined to the behaviour of flat circular footings on sand under inclined and eccentric loading.

The practical situation of a jack-up rig that one is attempting to model is illustrated in Fig. 1. That is the jack-up rig is floated onto the drilling site, the legs are lowered to the sea bed raising the platform (hull) above the sea surface and then preloading the foundations (spuds) by ballasting the hull with water.

The ballast (preload) is then removed prior to commencing drilling operations during which the foundations may be subjected to environmental forces such as wind, wave and tidal current, as well as the vertical self weight forces of the rig. This results in the footings being subject to vertical and horizontal forces P_v and P_h and to a moment M. A typical spud foundation is illustrated in Fig. 2. Although in the past many research workers have investigated the bearing capacity problem, e.g. Terzaghi, Meyerhof, Brinch-Hansen, Ticof Muhs and Weiss and many others.

The majority of this work has been conducted with small scale model footings at comparatively low stress levels thus the standard formulae involving bearing capacity factors in common use, quoted below in equation 1 have in general only been validated with data based on such models, there being very little data at sizes and stress levels appropriate to prototype scale footings and of course very little indeed appropriate to conical based footings.

$$q = S_c\, C\, N_c + S_q\, D\, N_q + \tfrac{1}{2}\, S_\gamma\, \gamma\, B\, N_\gamma \qquad (1)$$

where q is the vertical bearing capacity stress,

S_c, S_q, S_γ are footing shape factors

N_c, N_q, N_γ are the bearing capacity factors

for cohesion, surcharge, and self-weight respectively, and vary exponentially with the angle of internal friction ϕ,

C is the soil cohesion D is the depth of overburden and B is the breadth or diameter of the footing.

Typically S_c, S_q and S_γ have values of 1 for strip footings 1.2, 1, 0.4, respectively for square footings and 1.2, 1, 0.6 respectively for circular footings.

For the case of eccentric and inclined loading of strip footings on sand equation 1 is often modified as shown in equation 2 below.

$$q = \left(1 - \frac{2e}{B}\right)\left(1 - \frac{2\alpha}{\pi}\right)^2 \gamma D N_q + \left(1 - \frac{2e}{B}\right)^2 \left(1 - \frac{\alpha}{\phi}\right)^2 \tfrac{1}{2}\gamma B N_\gamma \qquad (2)$$

where e is the eccentricity at the point of action of the force on the base of the foundation measured from the centreline of the foundation and α (which must be less than ϕ) is the inclination of the force to the vertical (see fig. 3).

If such equations are to be of use for the case of full scale spud foundations then they need to be validated at appropriate stress levels for both flat and conical based footings.

The aim of this paper is to provide some of the data for such validations by presenting data from centrifuge model tests at stress levels more appropriate to full-scale footings. In addition data on the load displacement behaviour under eccentric and inclined loads will also be presented.

The Test Program

In view of the sparsity of data at different stress levels for flat based footings most of the tests were conducted with flat based circular footings. The program of tests that has been achieved so far is summarized in Table I.

The tests about to be described below were conducted on the Cambridge 10 m diameter Geotechnical centrifuge.

The tests covered vertical, horizontal and eccentric loading of 50, 75 and 100 mm diameter flat footings and vertical loading of a 120 mm diameter conical footing with an apex angle of 120° on dense Leighton Buzzard sand (BS 14/25).

Four sand specimens were prepared by pouring with voids ratios in the range of 0.47 to 0.49.

The footings were made from a duralumin alloy with a good quality machined finish giving a coefficient of friction with the Leighton Buzzard sand in the region of 0.20.

The loading system is illustrated in Fig. 4 and had a capacity of about 10 kN (≈ 2000 lb) vertically and 2.5 kN (≈ 500 lb) horizontally. Photographs of the apparatus may be seen in Fig. 5.

The tests were conducted at g levels covering the range 10 to 60 g. Thus in the case of the 50 mm diameter model footing this corresponded to prototype diameters in the range 0.5 to 3.0 metres.

The sand specimen container was 762 mm x 762 mm square in plan with a depth to the base of the sand of about 200 mm. (Bricks were placed in the bottom of the specimen container in order to reduce the amount of sand required to prepare a specimen). Due to the relatively restricted capacity of the loading system it was not always possible to fail a footing at the planned g level, as a consequence in many cases multi-stage tests were conducted, i.e. having yielded a specimen - say at 40 g and also having reached the maximum capacity of the loading system the load would be removed and the g level then reduced to say 20 g, and the footing reloaded to yield. Subsequently the g level may again be reduced to say 10 g and the footing again reloaded to yield and then eventually to failure. Typical loading paths are shown in Fig. 6.

Some Typical Results

Vertical loading

Initially it was necessary to explore the effects of stress level or the so-called scale effect. This was most easily achieved by considering the results obtained from tests S1, S3 and S2, which were conducted on 100, 75 and 50 mm diameter footings respectively. These footings were brought to failure at 1 g, 10g and 60 g, corresponding to footing prototype diameters of 01. m, .75 m and 3.0 m, respectively. In order to appreciate the very marked scale effects these results are presented in Fig. 7 as N_γ and N_γ* plotted against $Bn\gamma$ where N_γ* is given by $q = 0.5\ \gamma B N_\gamma$* and $S_\gamma N_\gamma = N_\gamma$*, B is the footing diameter, n is the number of gravities and γ the soil unit weight at 1 g. S_γ is taken as 0.6 for a circular footing. Also indicated in this figure for comparative purposes are the results of Terashi et al (1984) and King et al (1984).

All of the results indicate a very marked scale effect and in the case of the present authors' results going from a 0.1 m diameter footing to a 3 m diameter footing reduces the N_γ values by a factor of 3 which corresponds to a reduction of ϕ of about 6°.

Since the restricted capacity of the loading system did not allow a satisfactory modelling of models at failure, such modelling of models was restricted to investigating load displacement behaviour. Load displacement results from the same three tests, i.e. S1, S3 and S2 carried out at 30, 40 and 60 g i.e. corresponding in each case to a 3.0 metre diameter prototype are presented in Fig. 8 in prototype terms.

If the modelling were perfect then instead of three slightly different curves that can be seen in the figure, there would only be one. Thus at first sight it appears that the world of geotechnical centrifuge modelling is indeed an imperfect one, however there are reasons why one might expect the curves to be slightly different. The main reason is possibly the influence of the boundaries of the container and in particular the influence of the depth of the sand layer (h_s) which was only .195 m which is comparable with the footing diameters, i.e. for model footing diameters of .1, .075 and .05 m the depth to footing diameter ratio ($^{h_s}/_B$) is 1.95, 2.60 and 3.9 respectively. Plots of the vertical stiffness $\bar{K}_v$ (where $\bar{K}_v = {}^{q_v}/_{(\frac{dv}{B})}$ and is

B times the slope in Fig. 8) against depth/diameter ratio h_s/B for first loading and reloading are shown in Fig. 9. It is evident that for both first loading and reloading that as the depth/diameter ratio decreases the soil foundation is apparently stiffer. Also indicated in this figure are curves based upon an elastic solution (Poulos & Davis 1968) allowing for the influence of a rigid base at finite depth. It therefore seems that the majority of the discrepancy between the three curves in Fig. 8 may be accounted for by the influence of the base of the sample container box. It is also apparent that in order to obtain a 'perfect' modelling of models it may be desirable to correctly scale the container as well as the model!

In respect of tests performed with eccentric and inclined loading some typical results (tests S7 and S8) are shown in Figs. 10(a) (b) (c). Three parameters are plotted in each figure against horizontal displacement, viz, the ratio of horizontal stress to vertical stress, the vertical displacement, and the rotation of the footing.

It is evident from the curves of q_h/q_v versus horizontal displacement that the behaviour is not precisely symmetric, however since positive values of eccentricity and inclination are smaller when plotting the data only the positive side of the loading loop will be considered. Fig. 11 shows the failure enveloped for horizontal load at zero eccentricity. Also presented are the data of Ticof (1977) and Muhs & Weiss (1973). The two bounding curves to the Ticof data are for $\frac{P_v}{P_v*} = \left(1 - \frac{\alpha}{\phi}\right)^2$ where $\alpha = \tan^{-1}\left(\frac{Ph}{P_v}\right)$ (3)

where P_v* is the vertical load capacity (P_v) at zero horizontal load (P_h) and zero eccentricity.

ϕ has been taken as 49° and 40° .

The line through the authors' data i.e. $\delta = 11.3°$ represents a reasonable lower limit to the centrifuge data obtained at 20 and 40 g. It is evident that most of these data points lie on the sliding limit of the envelope however the point at $P_v/P_{v*} = 0.5$ is at the changeover point to vertical bearing capacity failure as evidenced by the direction of the displacement vector.

Note that the footings used by James & Tanaka had a max δ value of about 11.3° corresponding to a friction coefficient of 0.2 whereas Ticof used rough sandpaper on the base of his footings allowing him to develop much larger δ values.

Fig. 12 is similar to Fig. 11 but now includes data and a failure envelope for the case of an eccentricity of 15 mm (footing diameter 75 mm $\therefore \frac{e}{B} = 0.2$).

The failure enveloped at e = 15 mm has been obtained from

$$\frac{P_v}{P_v^*} = \left(1 - \frac{2e}{B}\right)^2 \left(1 - \frac{\alpha}{\phi}\right)^2 \qquad (4)$$

and has been evaluated for $\phi = 40^\circ$. - Again most of the data points lie in the sliding failure range however the displacement vectors at $\frac{P_v}{P_v^*} = .25$ and .345 indicate a changeover into the vertical failure mode.

Thus from the present data, albeit very limited, it appears that the failure envelope defined by $\frac{P_v}{P_v^*} = \left(1 - \frac{2e}{B}\right)^2 \left(1 - \frac{\alpha}{\phi}\right)^2$ for eccentric and vertical load seems conservative, provided the lower portion of the envelope is cut off by the line $\frac{P_h}{P_v^*} = \frac{P_v}{P_v^*} \tan \delta$ ~

The validity of the eccentricity yield locus i.e. $\frac{P_v}{P_v^*} = \left(1 - \frac{2e}{B}\right)^2$ is of course supported by the findings of many other workers and here in Fig. 13, Fig. 17 of Terashi et al (1984) is reproduced, demonstrating clearly that this expression is a reasonable lower limit estimate.

Conical Footing Results

Typical results of the tests on the 120 mm diameter conical footing are shown in Fig. 14.

The hollow circles are for the total vertical load P against vertical displacement and the solid black circles are the average vertical stress q* i.e. $q^* = P/A_s$ where A_s is the area of a plane section through the cone at the level of the sand surface.

There is a difficulty on the centrifuge in establishing the complete loading displacement relationship for a cone since with a simple experimental arrangement it is necessary to start the test with an initial vertical embedment of the cone of some 20 to 30 mm, which

in prototype terms say for a 100^{th} scale model could represent 2.0 to 3.0 metres! In order to circumvent this problem multistage tests were performed, i.e. the cone was penetrated at 40 g from .0205 m to .0215 m (at which displacement the full capacity of the loading system was reached). This is plotted in prototype terms in Fig. 15 on the curve labelled 40 g, i.e. upto a load of about 3.5 MN the displacement remains steady at .82 m (.0205 x 40), then yield occurs and the vertical displacement increases to 1.1 m (.0275 x 40) at which point the cone is unloaded and the centrifuge acceleration reduced to 20 g thus in effect giving us a smaller prototype cone at a smaller embedment. That is the 20 g penetration test now commences at a vertical embedment of .55 m (.0275 x 20) yield occurs at about 2.0 MN vertical load and the displacement increases to 0.6 m (.03 x 20). The cone is now unloaded and the procedure repeated at 10 g. Each time yield is reached we may consider that we are back on the virgin loading curve and thus the dashed line in this figure may be considered as the virgin load dispalcement curve for such a cone. The 60 g curve on the righthand side of the figure was obtained from the results of Silva Perez (1983). The chain dotted line in this figure is calculated employing experimentally determined N_γ values from the flat footing tests and is for the equivalent flat footing, i.e. treating the plane section of the cone level with the soil surface as a surface footing. It is apparent for this particular case that the cone has approximately $\frac{1}{4}$ the capacity of the equivalent flat plate.

Conclusions

Initial exploratory centrifugal testing of circular footings on sand indicate a very strong dependence of the self weight bearing capacity factor N_γ on stress level. The failure locus given by the expression $\frac{P_v}{P_v^*} = \left(1 - \frac{2e}{B}\right)^2 \left(1 - \frac{\alpha}{\phi}\right)^2$ appears to be conservative however the lower portion of the yield locus must be cut off by a straight line $\frac{P_h}{P_v^*} = \frac{P_v}{P_v^*} \tan\delta$ where $\tan\delta$ is the coefficient of friction between the footing and the sand.

Modelling of Models with respect to the load displacement behaviour of a 3.0 m diameter prototype flat footing gave a "satisfactory" correlation. Initial results for conical footings indicate that in this particular case, i.e. a 120° cone angle and $\delta \simeq 11°$ the vertical bearing capacity is about ¼ of that of the equivalent flat plate at the surface.

Acknowledgements

The Authors wish to thank the S.E.R.C. for providing funds, the Engineering Department for providing faiclities, there colleagues for assistance and encouragement, the P.R.H.I. of Yokosuka, Japan for enabling H Tanaka to spend a year at the C.U.E.D., and Professor J. A. Cheney of Davis University, California, who organized the Geotechnical centrifugal modelling symposium at which this paper was presented. Finally we extend our thanks to Reveria Wells for typing the manuscript.

References

Hansen, Bent, (1976) Modes of failure under inclined eccentric loads, Proc. of the first Int. Conf. Behaviour of off-shore structures, Vol. 1, pp 488-500.

Hansen, Brinch (1970) A revised and extended formula for bearing capacity, Bulletin, No. 28, The Danish Geotechnical Institute, pp 5-11.

King, G. J. W. et al. (1984) The development of a medium-size centrifugal testing facility. The application of centrifuge modelling to geotechnical design. Edited by Craig, W. H., University of Manchester, pp 25-46.

Meyerhof, G. G. (1953) The bearing capacity of foundations under eccentric and inclined loads, Proc. 3rd Int. Conf. Soil Mech. Foun. Eng., Vol. 1, pp 440-445.

Muhs, H and Weiss, K. (1973) Inclined load tests on shallow strip footings, Proc. 8th Int. Conf. Soil Mech. Foun. Eng., Vol. 1, Part 3, pp 173-179.

Perez, A. S. (1982) Conical footings under combined loads, M Phil thesis, University of Cambridge.

Poulos, H. G. and Davis, E. H. (1974) Elastic solutions for soil and rock mechanics, John Wiley and Sons. Inc.

Terashi, M. et al (1984) Bearing capacity of sand under eccentric load, Unpublished.

Terzaghi, K. (1943) Theoretical soil mechanics, Wiley.

Ticof, J. (1977) Surface footings on sand under general planar loads, Ph.D. thesis, University of Southampton.

Test No.	Footing type *)	dia.of footing (mm)	e	preload (MN/m^2)	ground No.	void ratio	unit weight (kN/m^3)	loading **)
S-1	F	100	0	0	1	0.489	17.87	V
S-2	F	50	0	0	1	0.489	17.87	V
S-3	F	75	0	0	2	0.487	17.89	V
S-4	F	75	10	2.2 e=0	2	0.487	17.89	V E
S-5	F	75	20	2.3 e=0	3	0.490	17.85	V E
S-6	C	120	0	0	3	0.490	17.85	V
S-7	F	75	0	0	4	0.471	18.08	V H
S-8	F	75	15	1.8 e=15mm	4	0.471	18.08	VHE

*) F = Flat footing
C = Conical footing

**) V = vertical loading
E = eccentric loading
H = horizontal loading

TABLE I - SAND TESTS

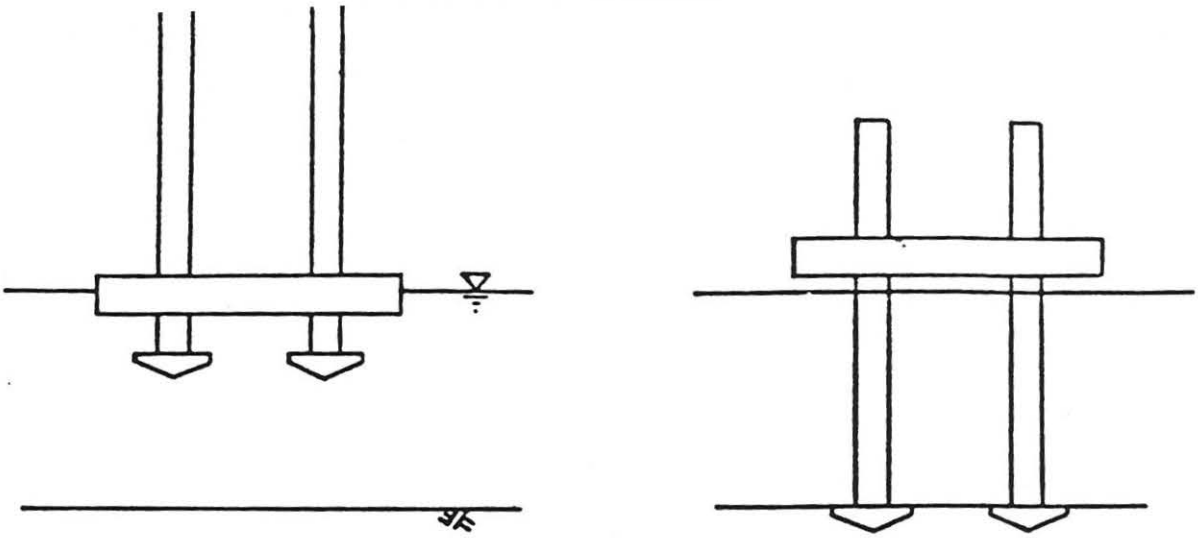

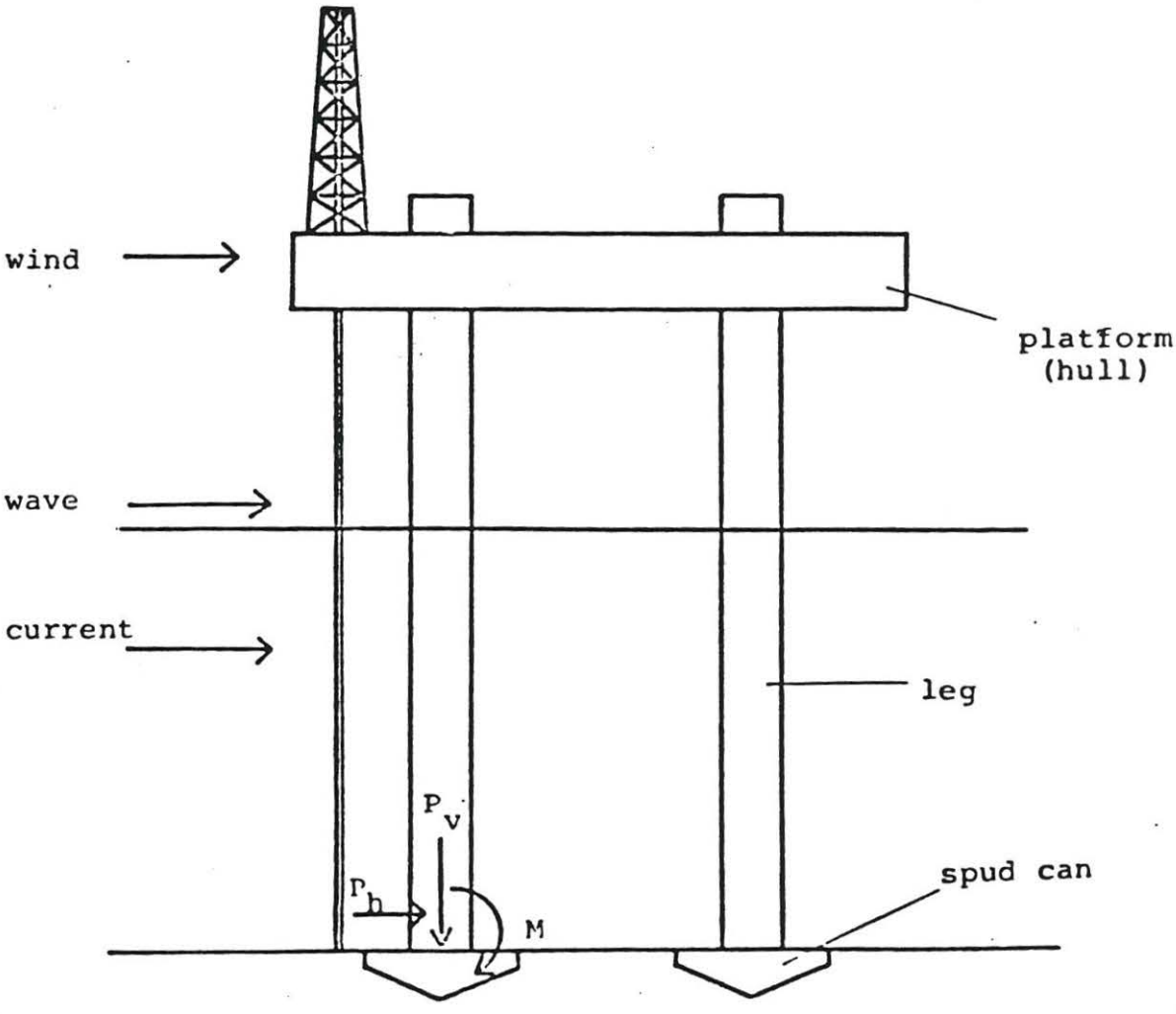

Fig. 1 jack-up rig

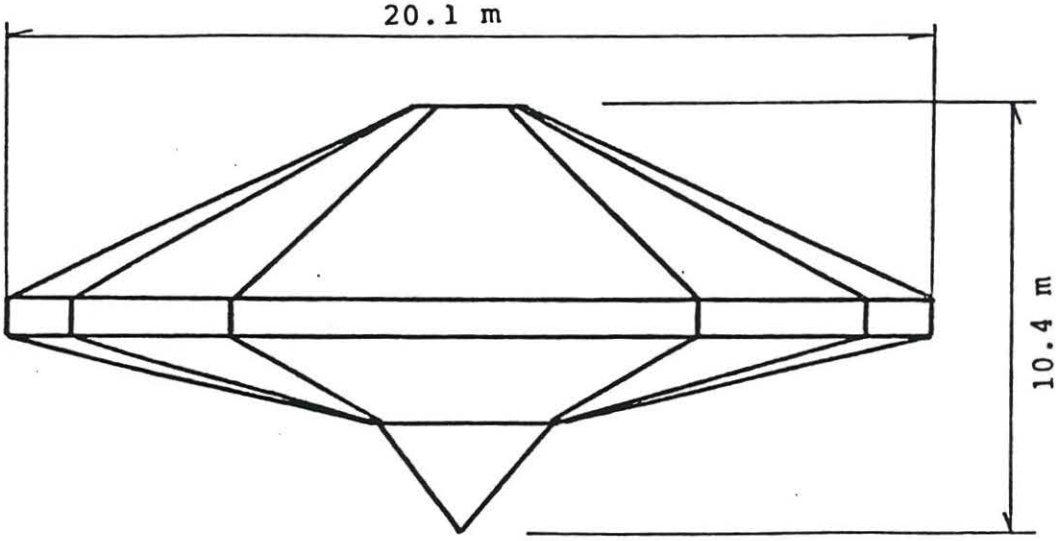

Fig. 2 spud can of jack-up rig

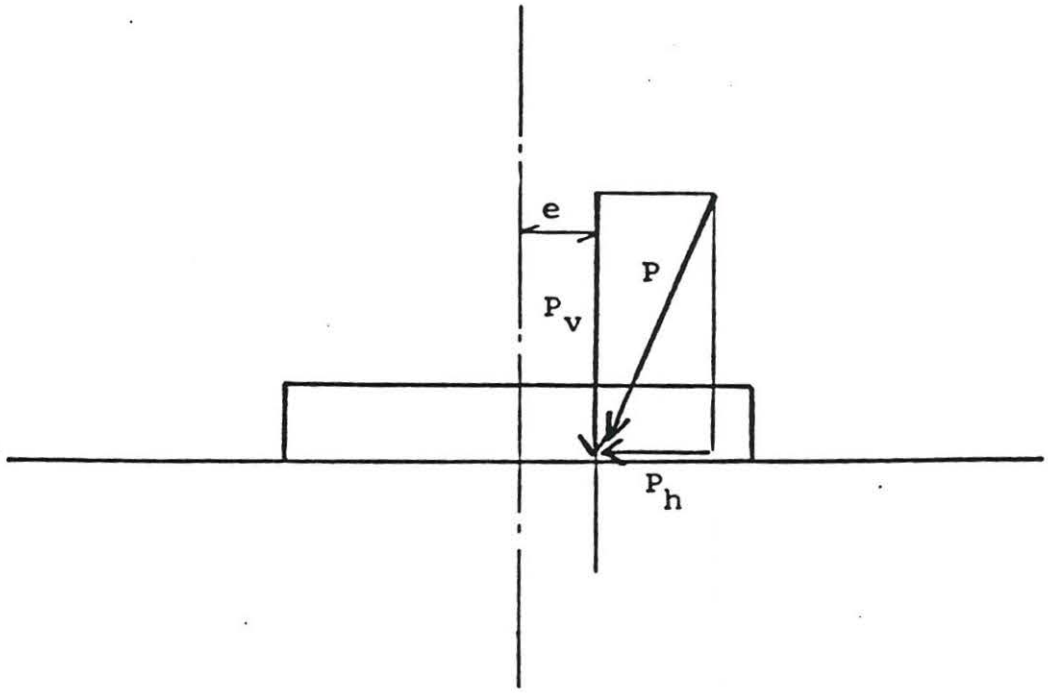

Fig. 3 eccentric and inclined load

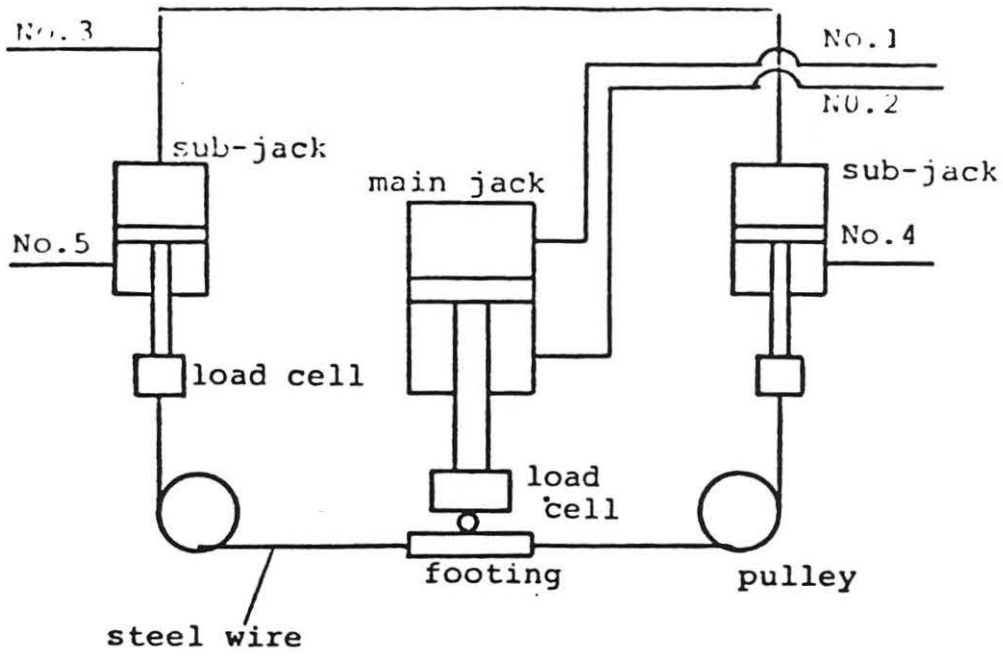

Fig. 4 . conceptual illustration of loading apparatus

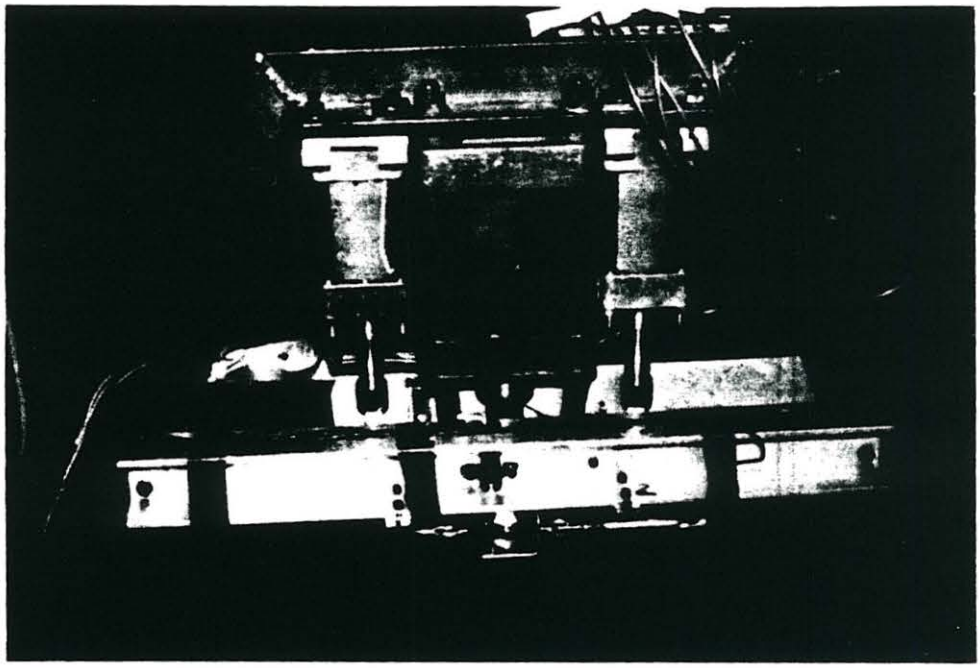

Fig. 5. Photographs of the footing apparatus

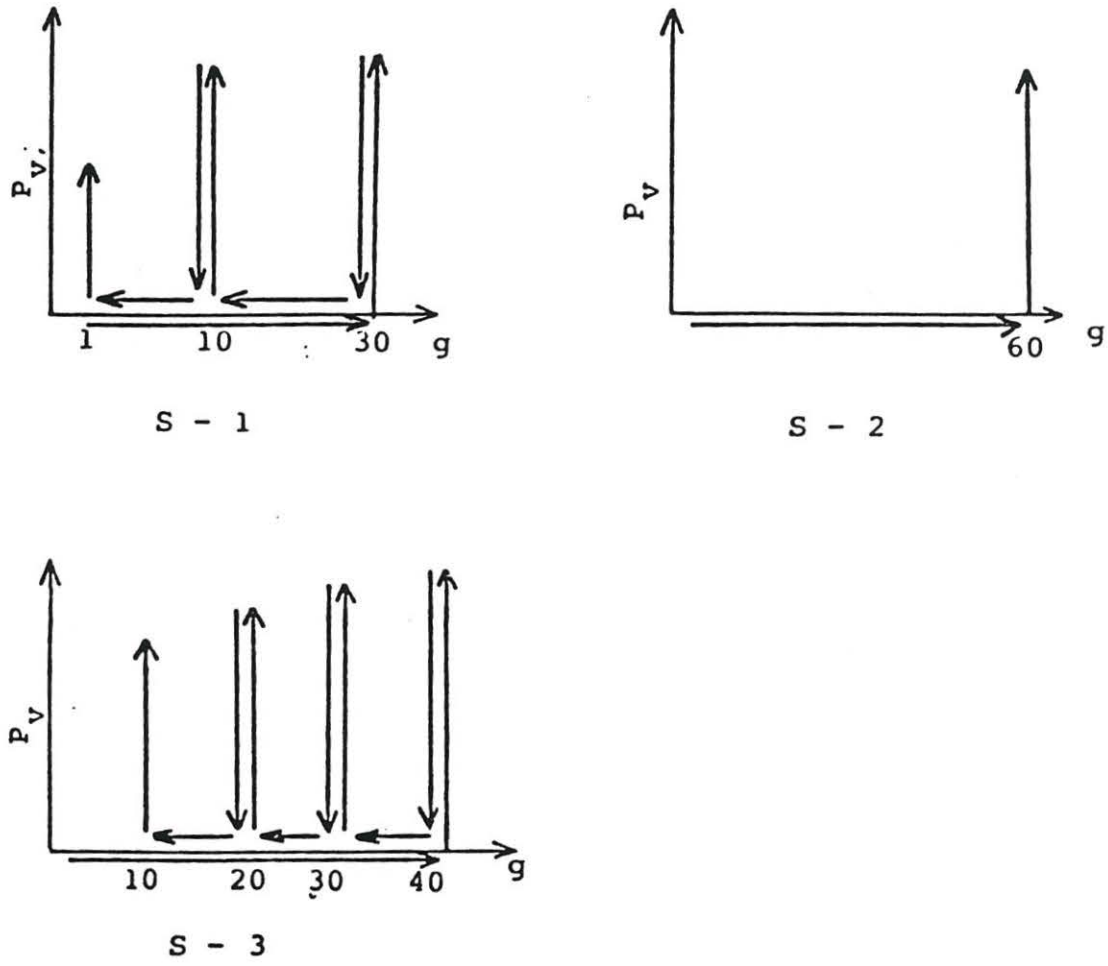

Fig. 6(a) loading path in tests S1 - S3

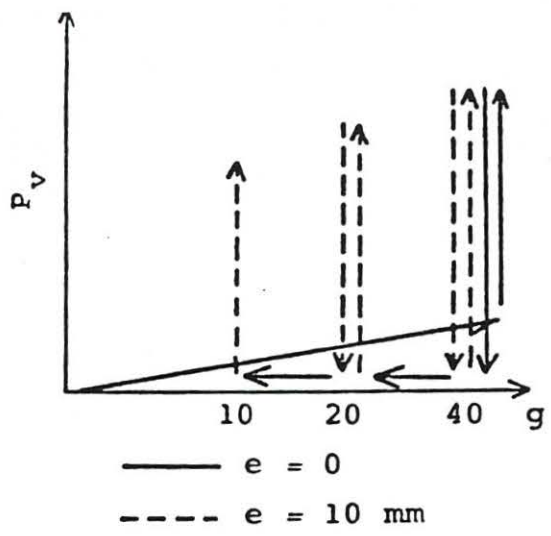

S - 4

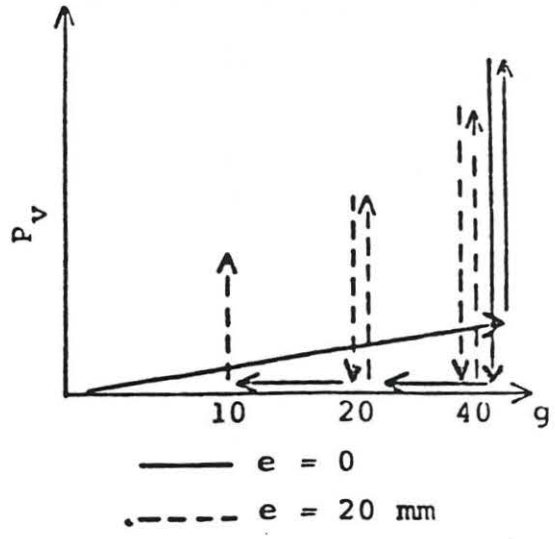

S - 5

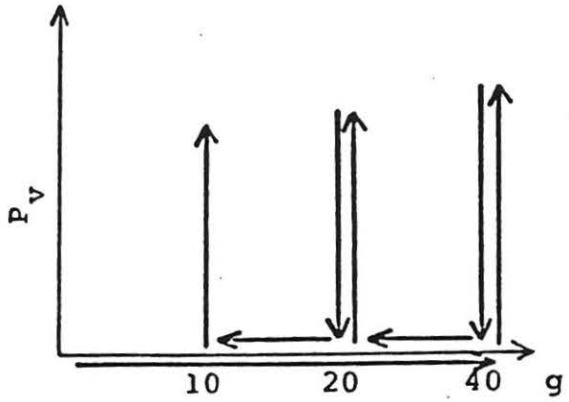

S - 6

H horizontal loading

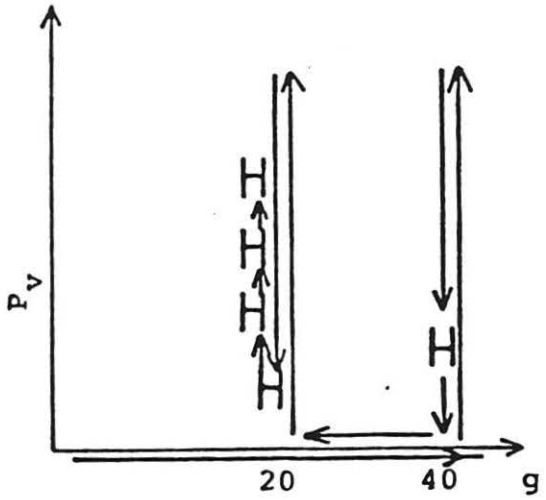

S - 7

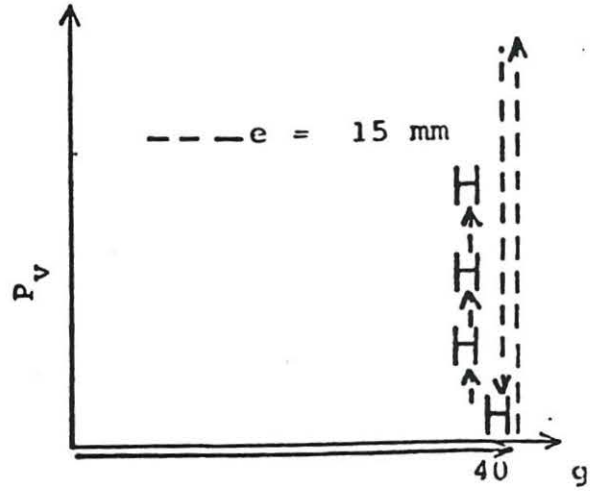

S - 8

Fig. 6(b) loading path in tests S4-S8

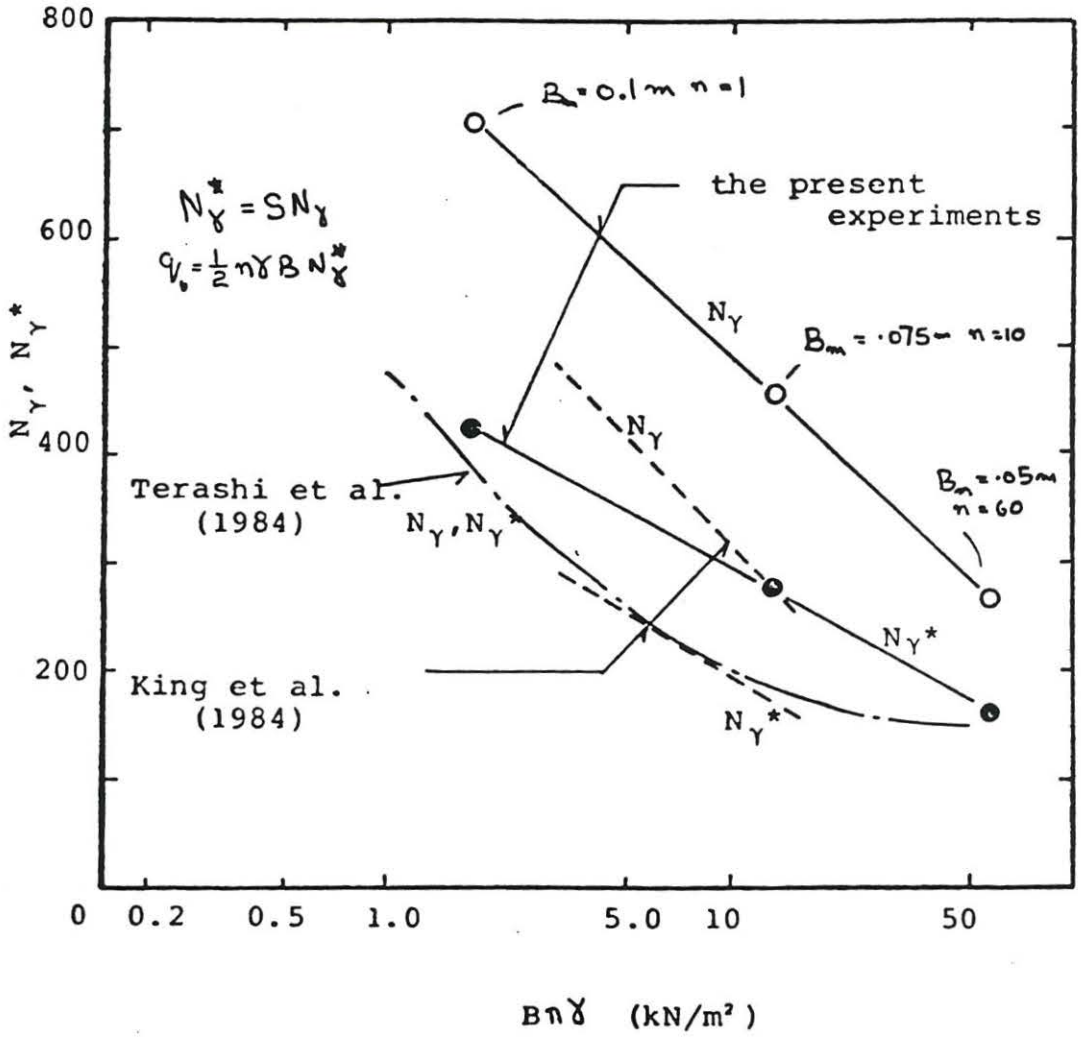

Fig. 7 influence of 'size effect' on bearing capacity factor N_γ

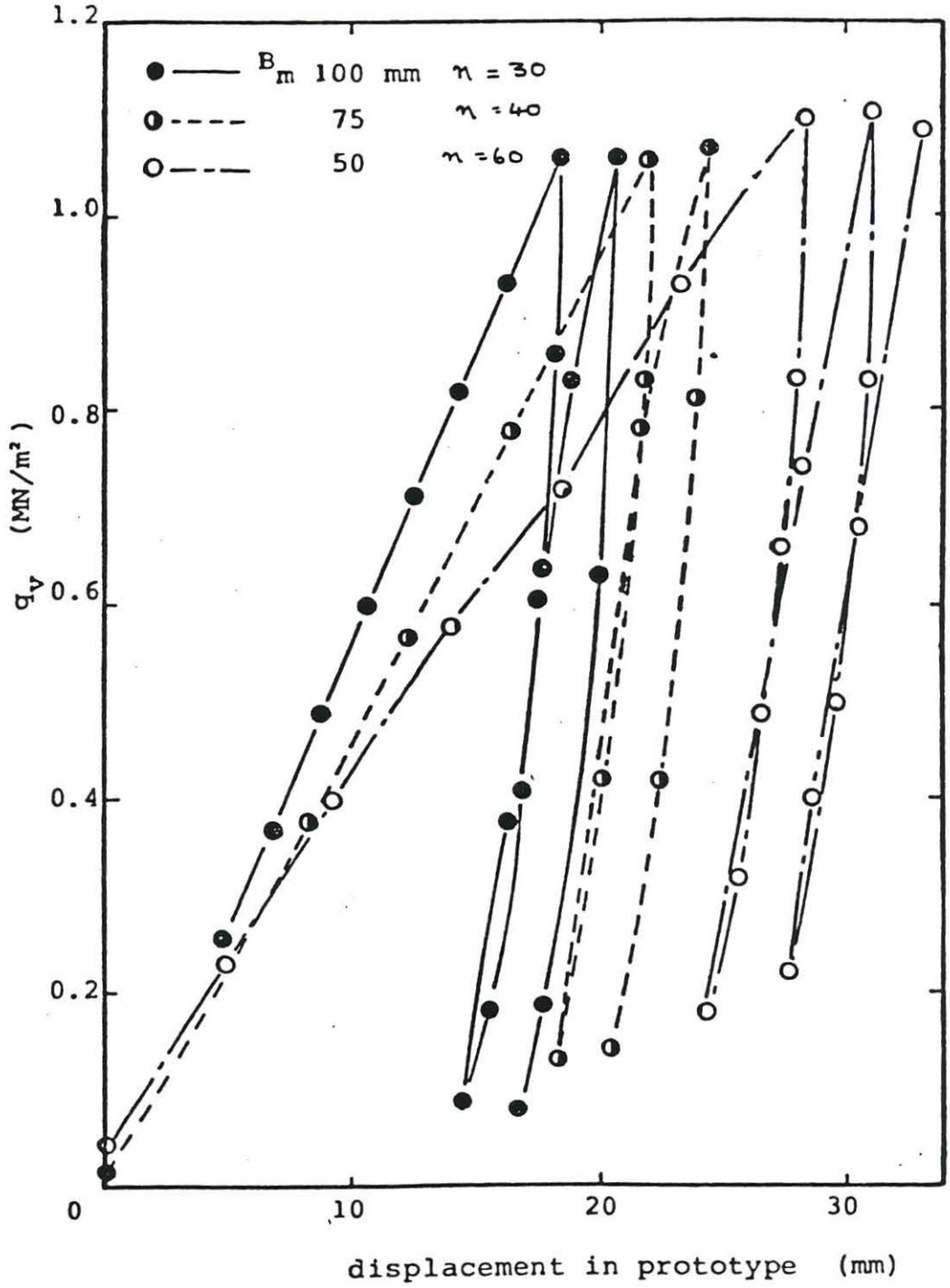

Fig. 8 modelling of models of bearing capacity on sand

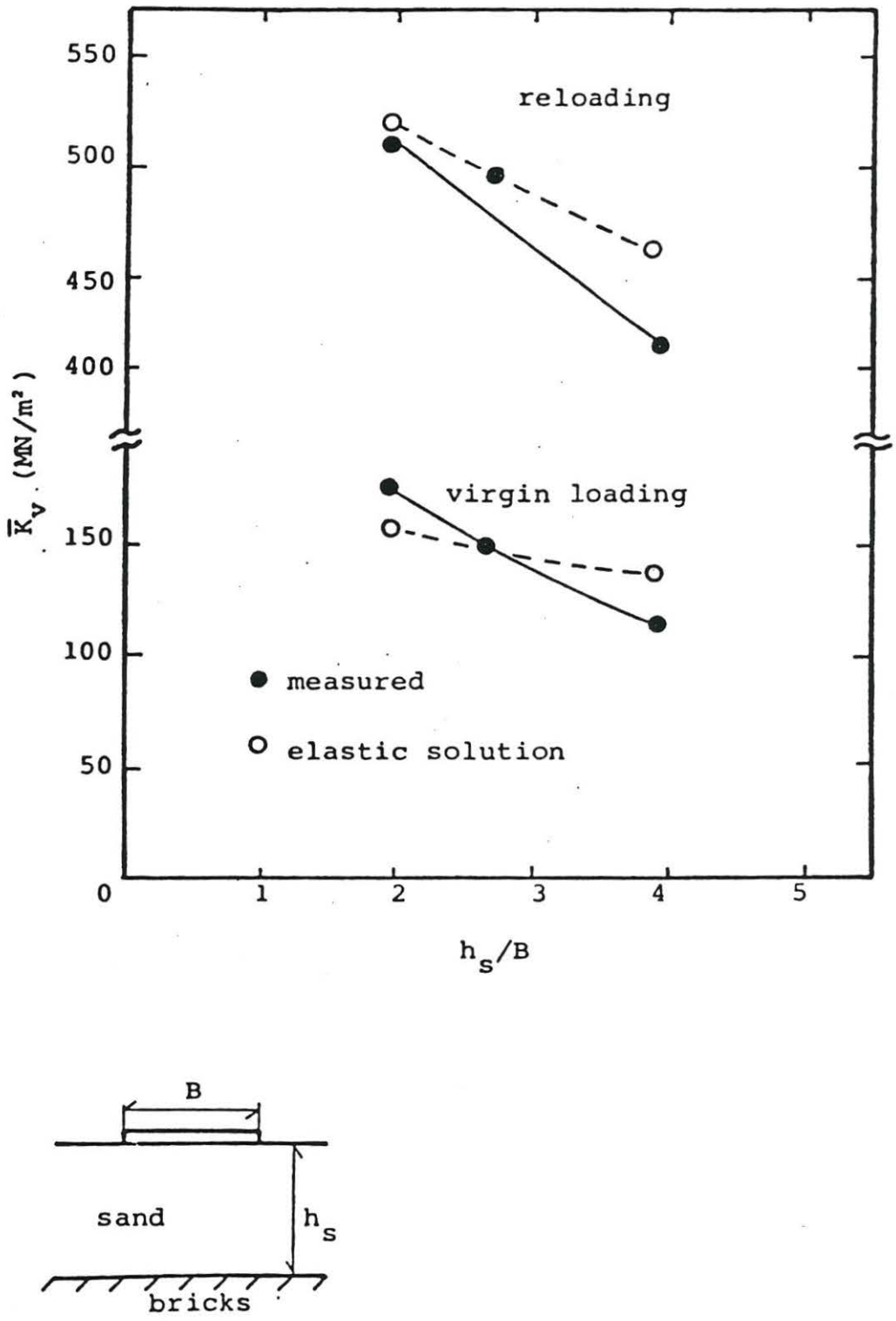

Fig. 9 influence of the existence of hard layer on coefficient of subgrade reaction

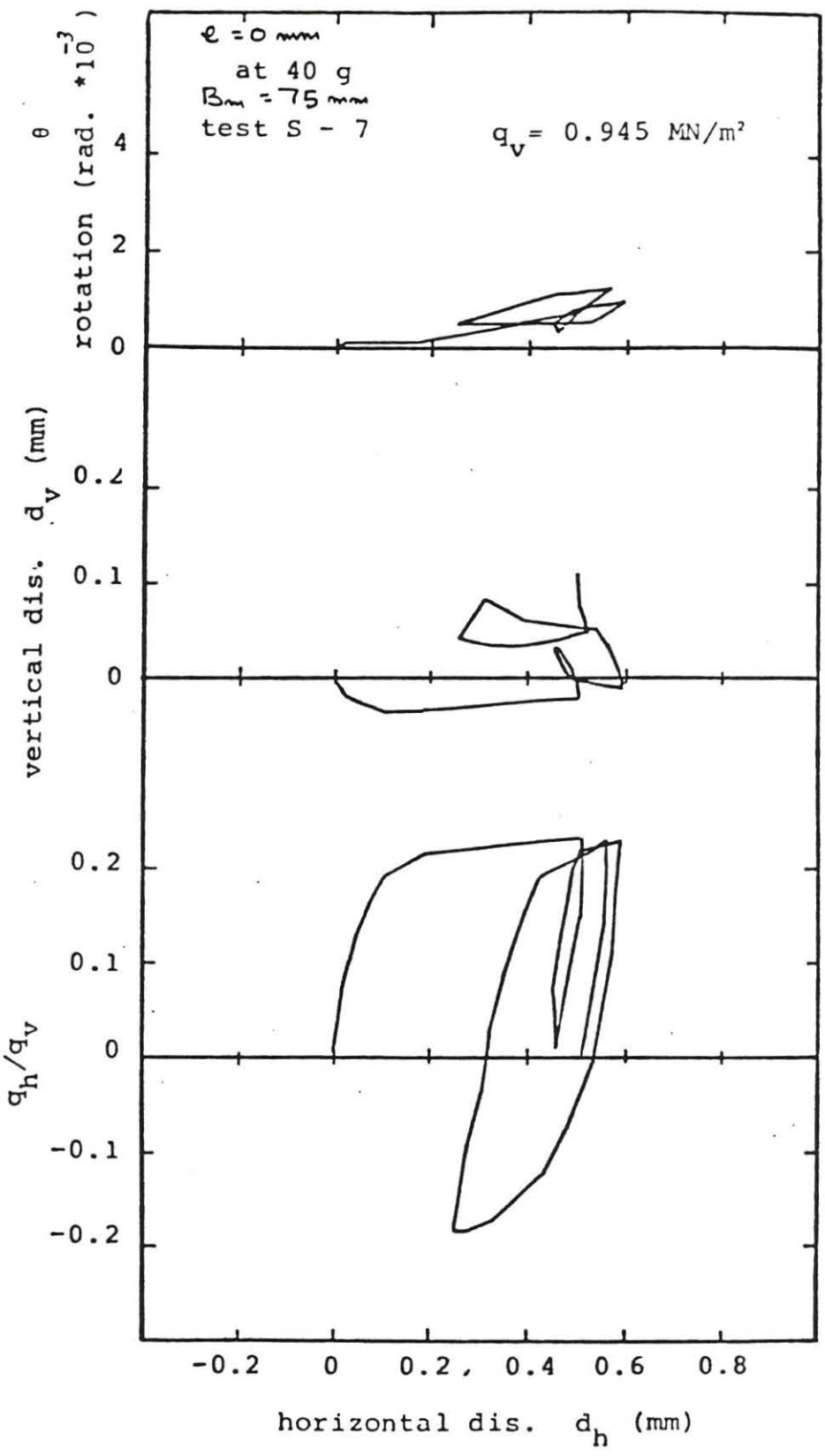

Fig. 10 (a) behaviour of footing under horizontal load no eccentricity

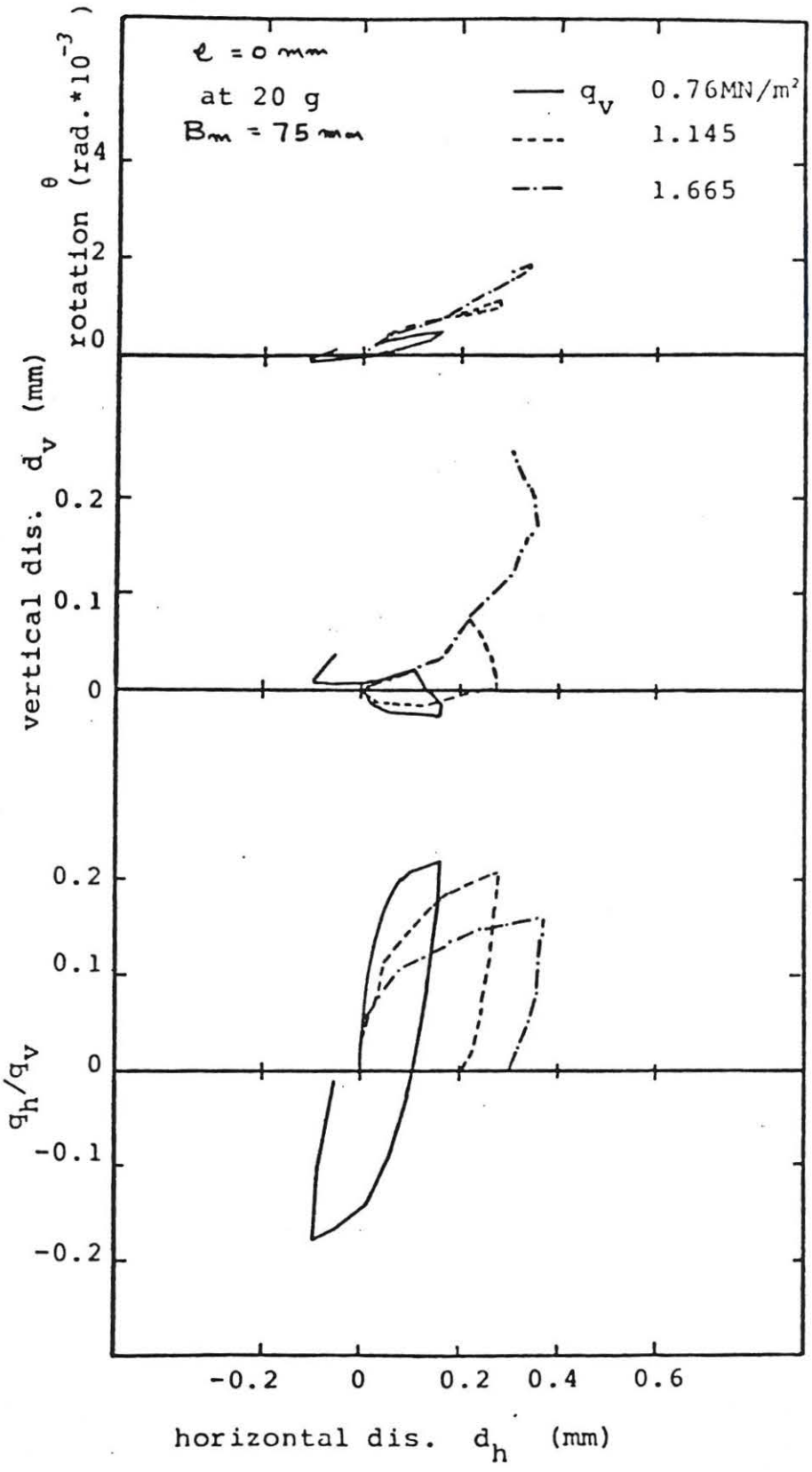

Fig. 10 (b) behaviour of footing under horizontal load no eccentricity

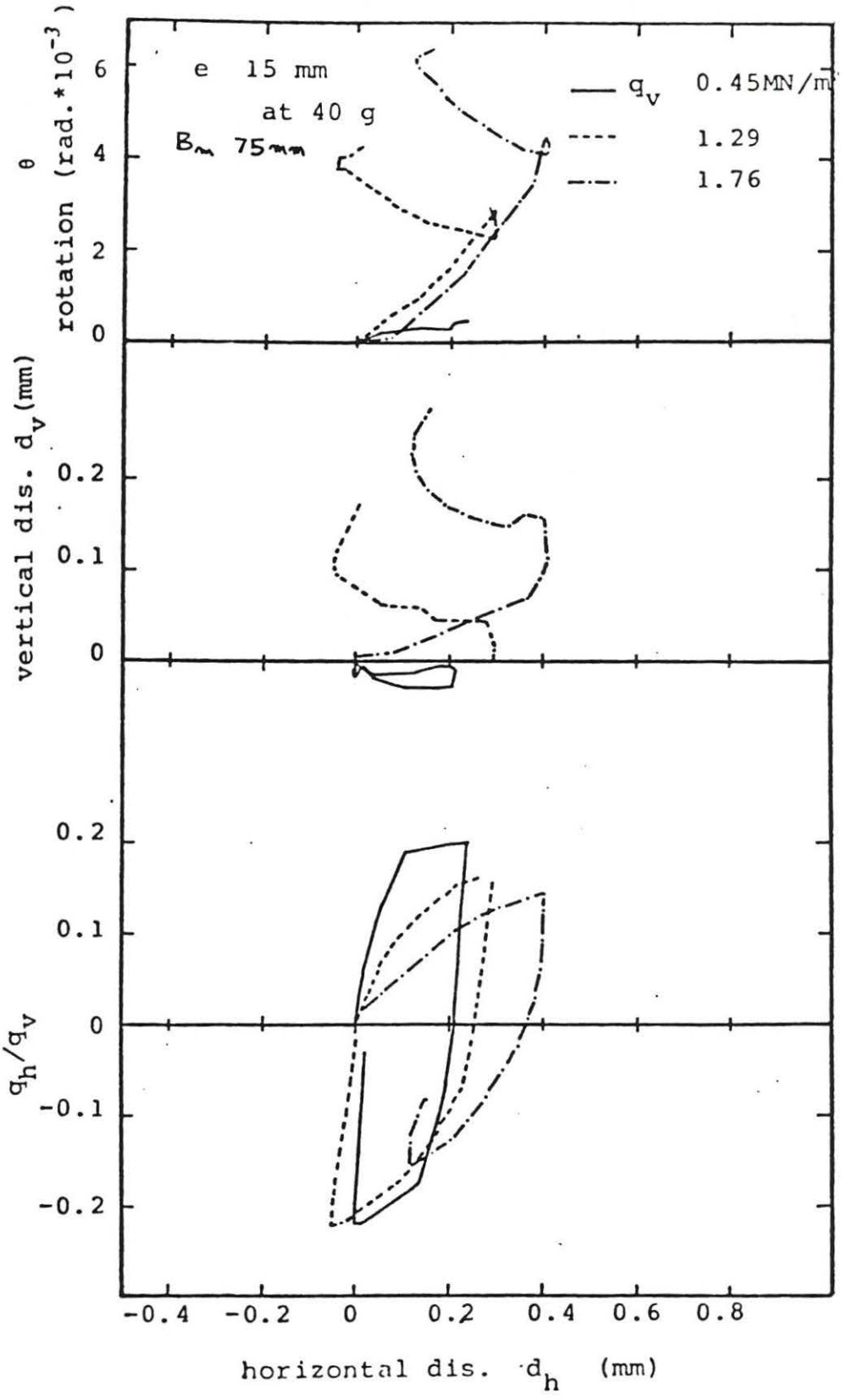

Fig. 10 (c) behaviour of footing under horizontal load eccentricity is 15 mm

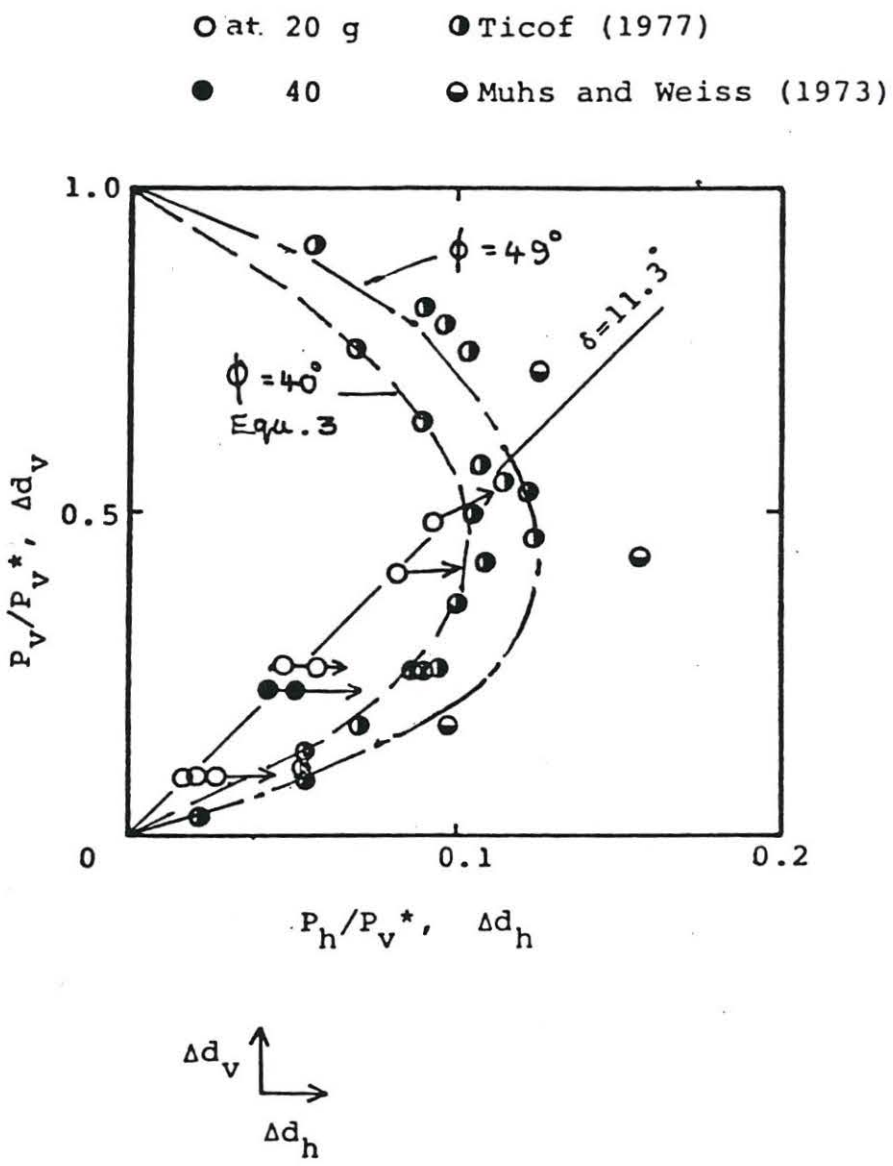

Fig. 11 failure envelope of horizontal load
no eccentricity

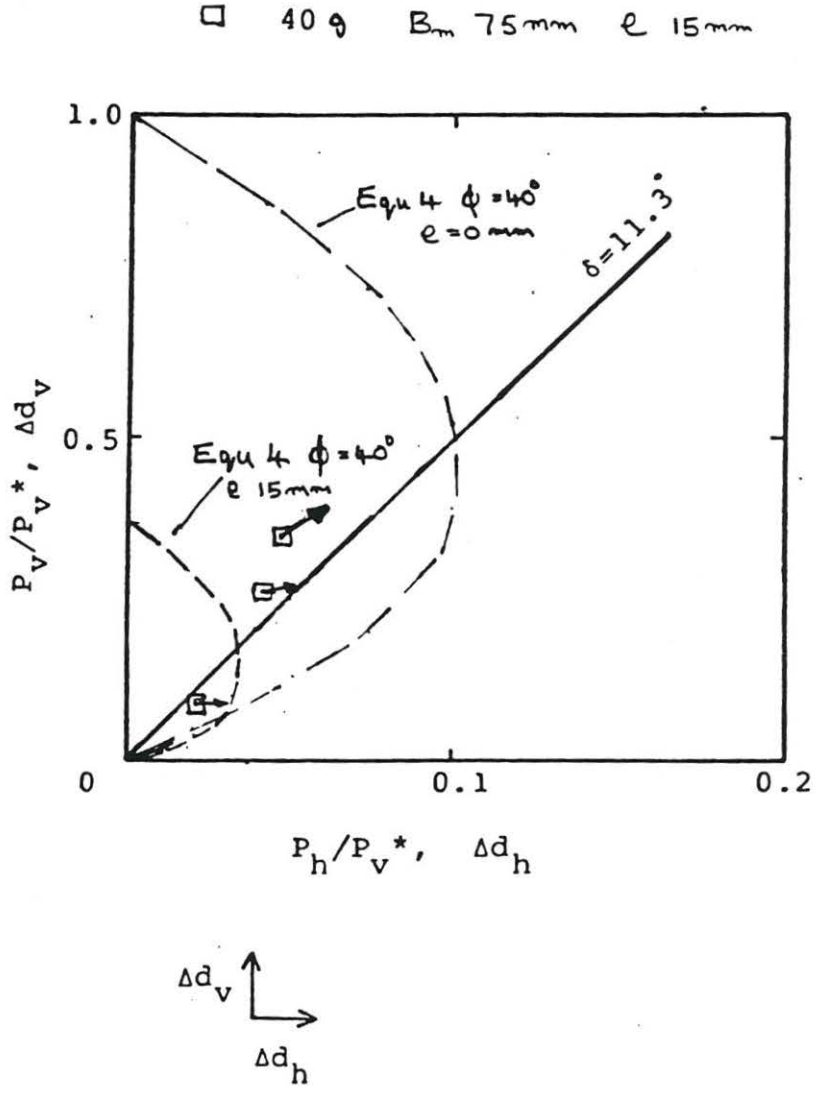

Fig. 12 failure envelope of horizontal load, eccentricity 15 m.m.

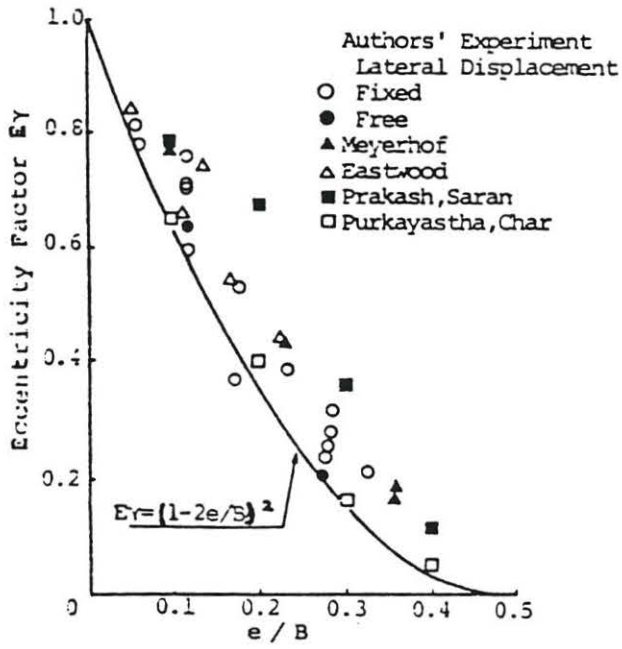

Fig. 17 Ey vs e/B

FIG. 13 ECCENTRICITY FAILURE 'LOCUS' (TERASHI et AL 1984)

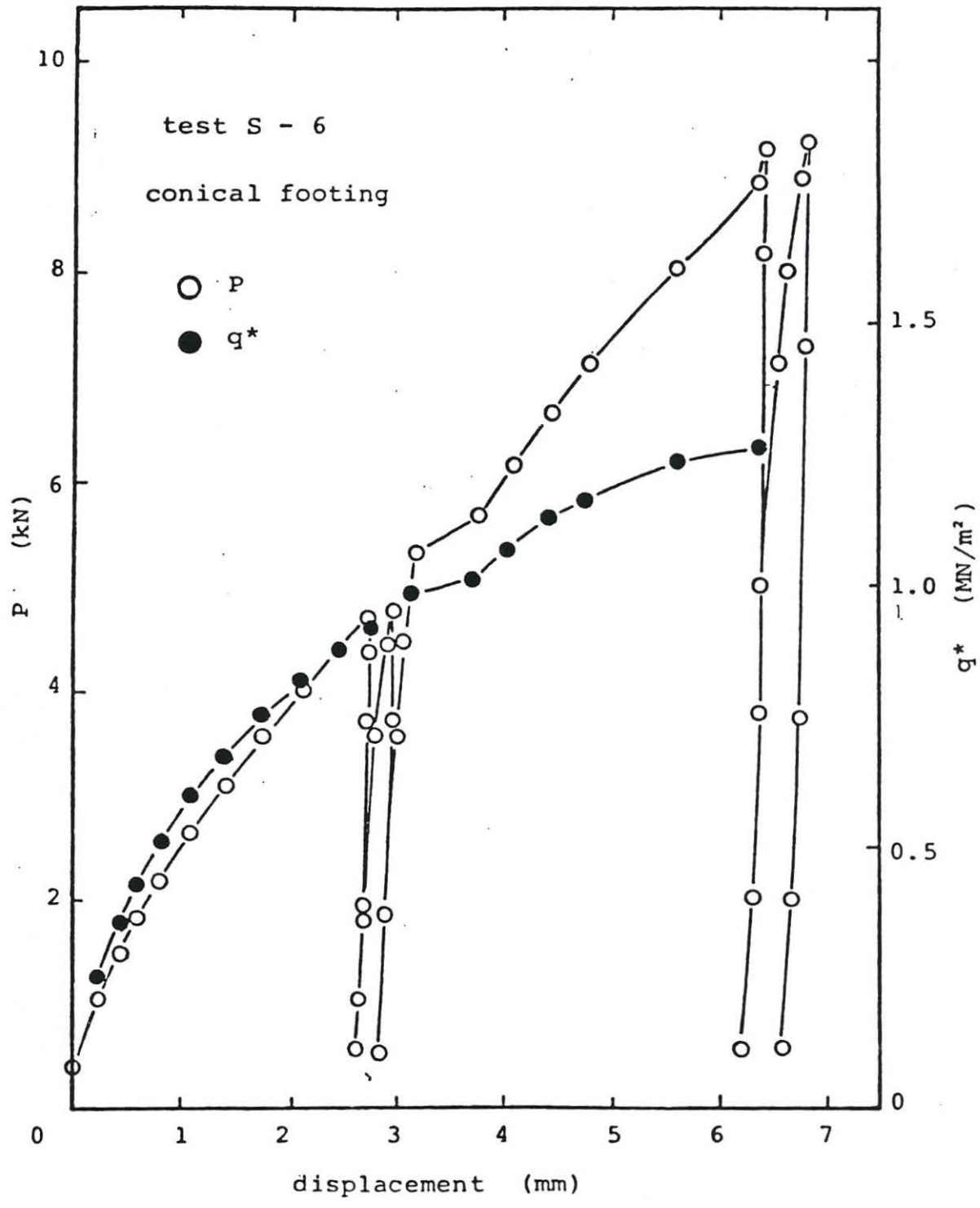

Fig. 14 relationships between force and displacement conical footing

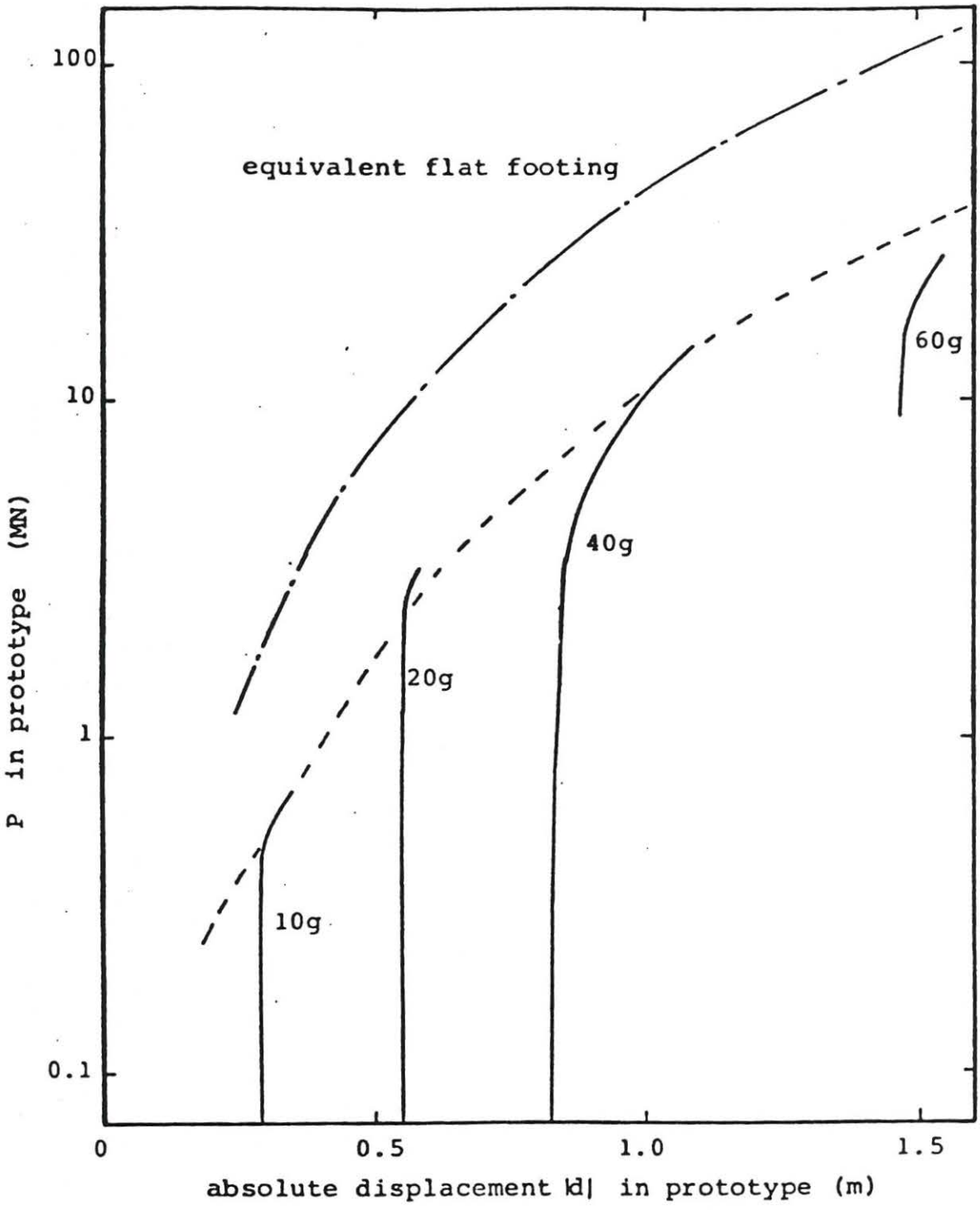

Fig. 15 relationships between force and absolute displacement in conical footing